World Academy of Science, Engineering and Technology
International Journal of Mechanical and Mechatronics Engineering
Vol:7, No:5, 2013

Predicting Crack Initiation Due to Ratchetting in Rail Heads Using Critical Element Analysis

I. U. Wickramasinghe, D. J. Hargreaves, D. V. De Pellegrin

***Abstract*—**This paper presents a strategy to predict the lifetime of rails subjected to large rolling contact loads that induce ratchetting strains in the rail head. A critical element concept is used to calculate the number of loading cycles needed for crack initiation to occur in the rail head surface. In this technique the finite element method (FEM) is used to determine the maximum equivalent ratchetting strain per load cycle, which is calculated by combining longitudinal and shear stains in the critical element. This technique builds on a previously developed critical plane concept that has been used to calculate the number of cycles to crack initiation in rolling contact fatigue under ratchetting failure conditions. The critical element concept simplifies the analytical difficulties of critical plane analysis. Finite element analysis (FEA) is used to identify the critical element in the mesh, and then the strain values of the critical element are used to calculate the ratchetting rate analytically. Finally, a ratchetting criterion is used to calculate the number of cycles to crack initiation from the ratchetting rate calculated.

***Keywords*—**Critical element analysis, finite element modeling (FEM), wheel/rail contact.

I. Introduction

WICKRAMASINGHE et al. [1] previously addressed the suitability of using accumulated plastic strain to assess the damage at the rail/wheel interface. As a result, relationships describing plastic equivalent strain with loading and friction were obtained. Further development using plastic strain components and failure criteria originally developed by Ringsberg [2] is used in the present research to calculate the number of cycles to crack initiation under ratchetting damage. The main problem involves identifying the critical element which coincides with the most likely region of crack initiation. The critical element is defined as the element in the finite element model which has the maximum equivalent ratchetting strain per load cycle, i.e. a combination of longitudinal strain and shear stain which shall be defined mathematically later on.

Ringsberg et al. [2] calculate the number of cycles to crack initiation under ratchetting failure using the critical plane concept they developed [3]. However, the procedure to identify the critical plane was not revealed in detail [2]-[6], making it difficult for other researchers to make inroads with this technique. The present research aims to address these limitations and devise new strategies for rail life prediction.

Rolling contact fatigue (RCF) failure in railheads has become an increasing problem in the railway industry over the years. Rising demand means that rail transportation must carry ever-increasing loads at higher speeds. Rail material is repeatedly loaded by train bogies as the train passes over the rail track. The maximum contact pressure that the rail material is able to withstand under elastic deformation is called the shakedown limit. The behavior of a material under cyclic loading during rolling/sliding can take four different forms, as illustrated in Fig. 1.

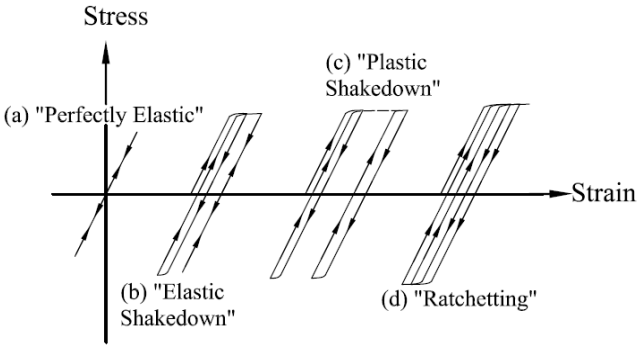

Fig. 1 Illustration of different material responses that occur for a material subjected to cyclic loading [4]

Analysis of various rail cross-sections in service shows that the material close to the contact surface at the rail head accumulates plastic shear strain. Depending on the actual loading conditions and the type of rail steel used, the thickness of this deformed layer varies from a few microns to a few millimeters. The response of the ductile material to a repeated cycle of loads depends on the magnitude of the applied load. If the applied load is below the elastic limit of the material, then the load is supported completely elastically (Fig. 1 (a)). If the load is higher than the elastic limit but less than the material's elastic shakedown limit then there will be some plastic deformation during the early cycles. This mechanism is explained in Fig. 1 (b). During this process of plastic deformation, material will accumulate protective residual stresses as a result of the strain hardening process. Thereafter, the load will again be supported elastically [7]. In both these cases the rail is loaded under the elastic shakedown limit and the contact deforms elastically at the steady state, giving long rail life [8]. Failure may eventually occur due to high cycle fatigue.

When the load is greater than the elastic shakedown limit, there will be some plastic flow during each cycle (Fig. 1 (c)). If the load is less than the plastic shakedown limit then the cycle of plasticity is closed and there will be no accumulation

I. U. Wickramasinghe is with the Queensland University of Technology, Brisbane, QLD 4000, Australia (Phone: +61451996004; e-mail: udarawic@gmail.com).

D. J. Hargreaves and D. V. De Pellegrin are with the Queensland University of Technology, Brisbane, QLD 4000, Australia. (e-mail: d.hargreaves@qut.edu.au, d.depellegrin@qut.edu.au).

of plastic strain. Therefore failure will occur by low cycle fatigue (LCF) [7]. When the applied load is higher than the plastic shakedown limit, plastic strain will accumulate. This process is referred to as plastic ratchetting Fig. 1 (d). The plastic shake down limit is also called the ratchetting threshold. Plastic ratchetting can lead to extrusion of thin slivers of material from the edges of the contact region causing 'lipping' of rails. Ratchetting is also the mechanism which causes large plastic shear strains observed in the near-surface material of the railhead [7]. These mechanisms are explained in detail by Kapoor [9]. This research focuses on the failure mode described in Fig. 1 (d) where ratchetting occurs.

Two main approaches are followed by researchers analyzing the rail-wheel contact. The semi-analytical approach mainly considers the elastic material properties, while finite element analysis (FEA) enables the elastic-plastic material properties to be studied. Semi-analytical approaches have an advantage over FE approach in terms of their simplicity and ability to analyze higher number of rolling passes. Several approximate methods have been developed, e.g. [10]-[12]. The main drawback of the semi-analytical method is the limitation of considering elastic material properties alone when plasticity dominates. Moreover, such approach usually involves a two-dimensional line contact solution, whereas real contacts are often best described in three-dimensions.

Finite element methods for analysis of rolling contact problems with elastic-plastic material models have been studied by several research groups [5], [13]-[16]. Finite element analysis results are considerably influenced by the type of material models used. Johansson and Thorberntsson [16] developed material parameters for the elastic-plastic material model using MATLAB optimization together with Bower's experimental results [17]. Their results formed the basis of the material model parameters used in Ringsberg et al.'s analysis [5].

Three-dimensional elastic-plastic finite element analyses of multiple rolling contact fatigue are not common in the literature. Ringsberg et al. [5] developed a finite element tool to successfully analyze the three dimensional wheel rail contact. In a previous study, Wickramasinghe et al. [1] developed a three-dimensional finite element model loaded with a Hertzian pressure distribution. The same loading method has also been used in the present research.

Rail steel failures occur as a result of the extreme demands of the rail industry, such as higher loads, greater traffic density and higher train speeds. Due to above listed behavior of materials there are two types of surface initiated cracks that appear on the rail head owing to rolling contact fatigue: head checks and squats. The objective of this research is to calculate the number of cycles to crack initiation with different traction conditions under ratchetting material failure conditions depicted in Fig. 1 (d). Numerous ABAQUS® [18] finite element analyses have been carried out using the elastic-plastic material model developed by the Schleinzer and Fisher [13] to analyze each scenario.

II. Numerical Modeling

A. Development of Pressure Loaded 3-D Finite Element Model

The three-dimensional rail model representing 80mm of track length is shown in Figs. 2 and 3. In this model, the train was assumed to roll on a straight track and it was assumed that the contact patch is located at the centre of the railhead. To identify the critical element and to capture high stress and strain gradients near the rolling contact surface, a fine mesh (higher mesh density) of 16x16mm cross sectional area was used near the contact surface. A total number of 27,136 eight-node brick elements were generated in the model using a mapped option, i.e. a so-called structured mesh. The mesh density of the inner part gradually decreases downwards form rail head surface to reduce the total number of elements of the model and reduce the computational time. The mismatch between the element meshes of the adjoining surfaces between the inner and outer parts is controlled using the ABAQUS "tie" constraint. This constraint causes adjoining surfaces to deform by equal measures. All the displacements of the bottom surface of the rail model and the displacements of the two ends of rail were constrained in the running (z) direction.

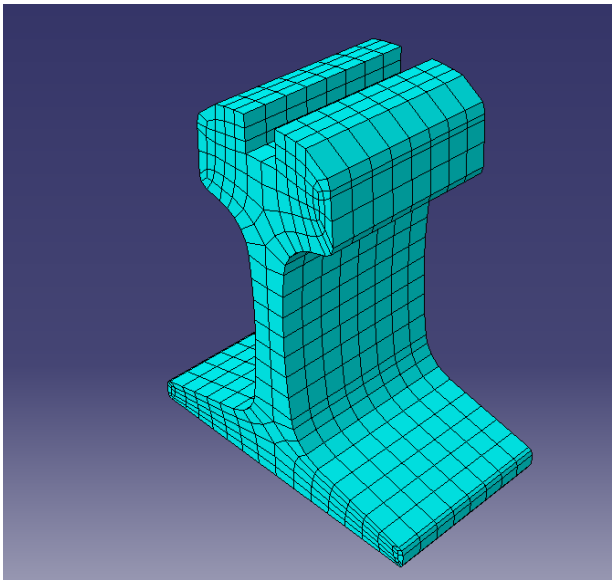

Fig. 2 Mesh of the rail body

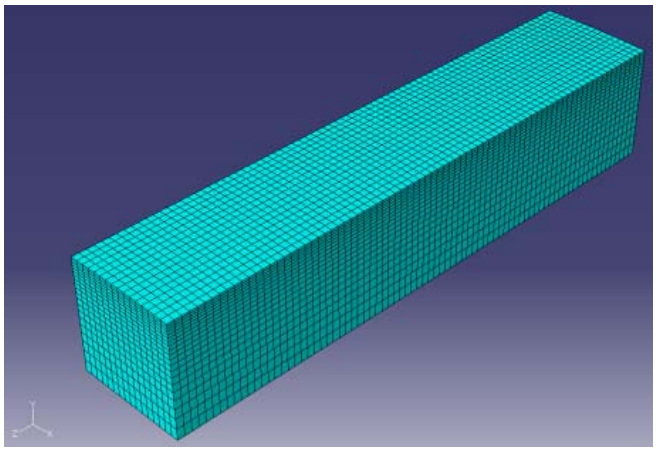

Fig. 3 Meshed rail insert

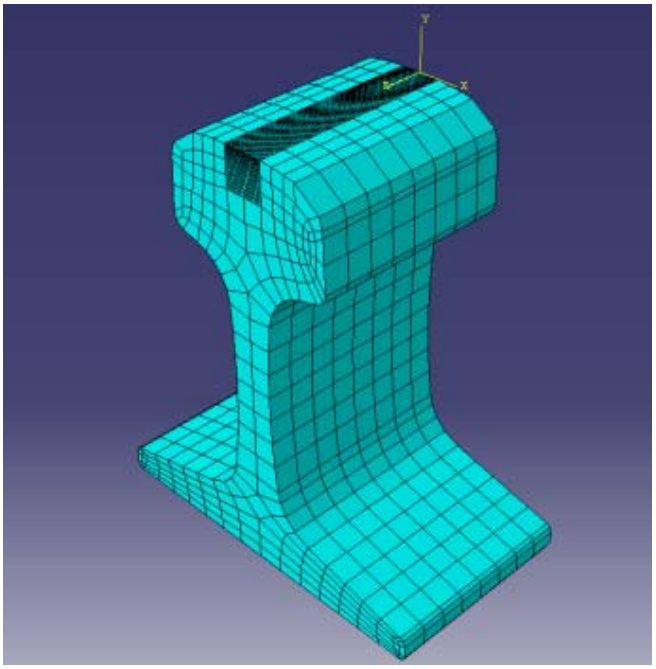

Fig. 4 The fully meshed rail

B. Load Application

The distributions of contact load and traction load arising in the wheel/rail contact were applied to the centre of the rail insert by using ABAQUS subroutines DLOAD and UTRACLOAD. In order to simplify the contact development, the analysis assumes single-point contact. During the analysis, a function using the coordinates as variables was used to describe the contact pressure as a Hertzian distribution. Therefore the 3-D Hertzian contact equations were used to define the contact ellipse semi-axes and the maximum contact pressure with the selected load condition [19], [20]. The chapter Contact and Creep-Force Models in Railroad Vehicle Dynamics [21] explains the procedure for calculating Hertzian parameters by assuming an elastic model for the wheel/rail contact.

C. Material Model

Only a thin layer of material in the vicinity of the wheel/rail contact region is expected to experience plastic deformation. Therefore, an elastic-plastic material model describes the material in the rail insert, since this is the volume within which plastic deformation is likely to occur as a result of the wheel/rail rolling contact. The rail base only experiences elastic deformation and is therefore modeled using a linear-elastic material model.

Material models are described by constitutive equations governing the stress / strain behavior of the material. In this research, the nonlinear isotropic/kinematic cyclic hardening model was used to define classical metal plasticity, as developed by Chaboche and Lemaitre [22]. In the Chaboche model, there are five material parameters (c, γ, b, Q_∞, σ_0) that need to be defined. These material parameters were found from the literature [4], [13]. The parameters were obtained by means of uniaxial cyclic tension-compression experiments on cylindrical specimens conducted by Bower [17] and Schleinzer and Fischer [13].

In the present study, the material properties were considered to be equivalent to British Standard BS11 normal grade steel as the experimentally verified material model parameters for this material were available in the literature: for example, Bower [17] carried out uniaxial experiments on normal grade BS11rail steel. From the generated results, several material models were developed to describe rail material behavior. Schleinzer and Fischer [13] performed experiments for UIC 900A rail material and developed a separate material model. Discrepancy between rails BS11 [23] and UIC 900A material properties were minor [2]. Wickramasinghe et al. [1] analyzed four different material models (Johansson and Thorberntsson [16]; Ringsberg et al. [5]; Ekh et al. [15]; Schleinzer and Fischer [13]) applied to normal grade rail steel and verified using the finite element model results that variations between the different models are minimal.

TABLE I
MATERIAL MODEL PARAMETERS FOR THE UIC 900A NORMAL GRADE RAIL MATERIAL FROM THE SCHLEINZER AND FISCHER MODEL

Material Constant	Value
σ_0 (MPa)	379
Q_∞(MPa)	189
$\gamma_1 \gamma_2 \gamma_3$	55, 600, 2000
b	500
$c_1 c_2 c_3$ (MPa)	24750, 60000, 200000
σ_0 (MPa)	379

Considering the fact that both UIC 900A and BS11 normal grade rail steel practically have similar behavior, material model parameters obtained by Schleinzer and Fischer [13] were used in the finite element analysis. Furthermore, this research has a significant improvement over the other three models as material parameters up to three back stresses have been published. Multiple back stresses significantly improve the analysis results in the plastic hardening phase. The various material model parameters considered for this research are provided in Table I.

III. Wheel/Rail Data and Loading Conditions

A. Rail Track and Wheel Dimensions

The rail and wheel dimensions for this research were taken from the literature [5]. The wheel radius of the locomotive is 0.46m and the transverse radius of the rail head is 0.3m. The rail track was considered to be straight and that contact occurs at the centre of the rail head.

B. Loading Conditions

The axle load considered for all scenarios was 26 tonnes, corresponding to a rail-wheel contact normal force of 130kN. The load was sufficient to initiate ratchetting deformation and in line with the industry norm. Different friction coefficients were analyzed to identify their effect on ratchetting damage. The friction force was calculated as a proportion of the normal force by multiplying the normal force by the friction coefficient. Exact values of the different loading conditions are provided in Table II.

TABLE II
Loading Conditions

Analysis No.	Load (kN)	Friction Coefficient	Calculated Maximum P_0 (GPa)
1	130	0	1.32
2	130	0.05	1.32
3	130	0.10	1.32
4	130	0.15	1.32
5	130	0.20	1.32
6	130	0.25	1.32
7	130	0.30	1.32
8	130	0.35	1.32

IV. Method for Calculation of Crack Initiation under Ratchetting Conditions

Fatigue life to crack initiation is studied using the strain-life approach [6]. This research addresses crack initiation due to rolling contact fatigue using the critical element rather than the critical plane approach [2].

A. The Critical Element Approach Combined with a Damage Accumulation Rule

Rolling contact load causes every element in the mesh to progressively increase its plastic deformation (ratchetting) with the number of cycles. The critical element has a maximum equivalent ratchetting strain per load-cycle which is determined using the critical element approach, described next.

B. Identifying the Critical Element from the FE Model

The method of identifying the critical element is similar to that used to calculate the equivalent ratchetting strain per load cycle. Ratchetting damage is calculated using the ratchetting criterion [24]. Crack initiation begins when the total accumulated strain reaches a critical value, ε_c, which is a material constant that depends on the ductility of the material. Once the material's total accumulated strain reaches ε_c, its ductility is exhausted, which is considered as the point of crack initiation [25].

Crack initiation in rail materials due to cyclic loading has been studied before [2]-[5]. The number of cycles to crack initiation caused by ratchetting, at load cycle n, can be calculated as,

$$\left(N_{f.rat}\right)_n = \frac{\varepsilon_c}{\left(\Delta\varepsilon_r\right)} \tag{1}$$

where $\Delta\varepsilon_r$ is the equivalent ratchetting strain per load cycle (ratchetting rate), calculated as

$$\Delta\varepsilon_r = \sqrt{\left(\Delta\bar{\varepsilon}\right)^2 + \left(\frac{\Delta\bar{\gamma}}{\sqrt{3}}\right)^2} \tag{2}$$

where $\Delta\bar{\varepsilon}$ is the plastic strain in the longitudinal (travelling) direction per load-cycle, and $\Delta\bar{\gamma}$ is the shear strain on the critical element per load-cycle. The material constant, ε_c, for BS11 normal grade rail material is 11.5[5]. The factors defining $\Delta\varepsilon_r$ are longitudinal strain and shear strain as per (1) and (2). Therefore, the history output of the set of 45 elements defined at the centre of the rail was examined to find the longitudinal and shear strain after every cycle, thus enabling identification the critical element.

Fig. 5 shows the defined set at the top of the rail to identify the critical element. Those elements with the highest shear and longitudinal strain must be included in this set.

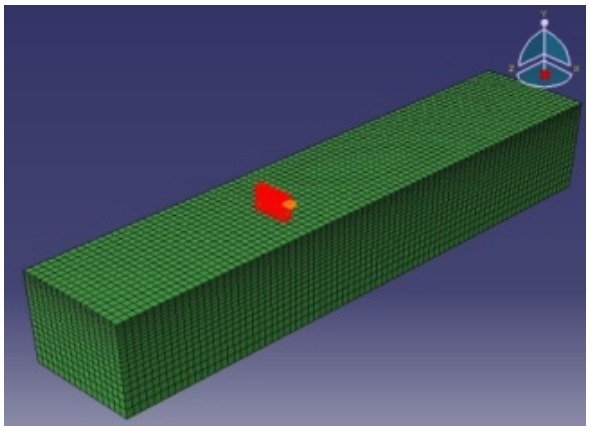

Fig. 5 Defined set to identify the critical element of the FEM

The history output data was collected for all the elements after the FEM analysis had completed 20 cycles. Longitudinal plastic strain, PE33, and plastic shear stain, PE12, values were extracted from FE analysis history data. The equivalent ratchetting strain per load cycle $\Delta\varepsilon_r$ was calculated using (2) for each element. The critical element was identified as that with maximum equivalent ratchetting strain per load cycle. This element represents the location where crack initiation is most likely to occur.

The equivalent ratchetting strain per load-cycle is higher during the initial cycles and causes very high plastic strain to

the critical element. Fig. 6 shows a typical per cycle equivalent ratchetting strain pattern with increasing number of cycles. It may be observed that as the number of cycle increases, the equivalent ratchetting strain per cycle becomes constant. Consequently, the number of cycles to crack initiation can be calculated with a modification of (1),

$$\left(N_{f.rat}\right)_n = \frac{\varepsilon_c - \varepsilon_{r0}}{\left(\Delta\varepsilon_r\right)} \tag{3}$$

where ε_{r0} is the aggregate of the equivalent ratchetting strain before the constant ratchetting rate. The aggregate ratchetting strain for the first 15 cycles was used as the measure of ε_{r0}. Therefore the effect of damage to the material during the early cycles will be eliminated when calculating the total number of cycles to crack initiation. That is, after 15 cycles the ratchetting rate for the material reached to a constant rate.

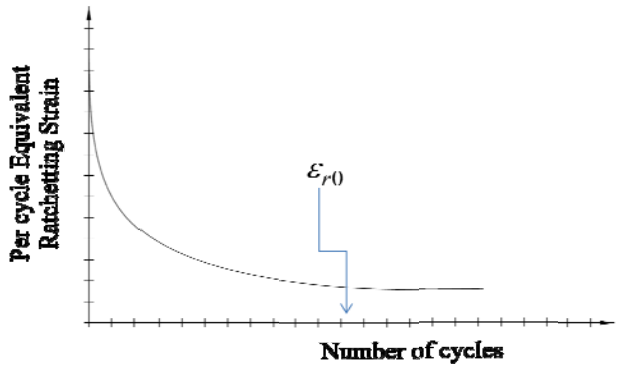

Fig. 6 Per cycle equivalent ratchetting strain changes with number of cycles

Finally, the number of cycles to crack initiation was calculated using the damage accumulation rule in (3). The damage was calculated on a per cycle basis and added linearly to the total damage.

TABLE III
ANALYZED RESULTS

Analysis No.	Friction Coefficient	No. of cycles to crack initiation (Thousands)	Calculated Maximum P_0 (GPa)
1	0	5433	1.32
2	0.05	4624	1.32
3	0.10	3284	1.32
4	0.15	2871	1.32
5	0.20	1757	1.32
6	0.25	38	1.32
7	0.30	21	1.32
8	0.35	3	1.32

V. Results and Discussion

A. Effect of Traction on the Ratcheting Fatigue Life of the Rail Material

The calculated number of cycles to crack initiation with different friction coefficients is summarized in Table III and plotted in Fig. 8. Wickramasinghe et al. [1] confirmed that the increase of friction coefficient causes material failure to move towards the rail surface as per the shakedown map in Fig. 7. Therefore, the material element in which the crack initiates varies from analysis to analysis. During the last two analyses (numbers 7 and 8), the critical element was at the rail surface whereas it was at near surface in analysis number 6.

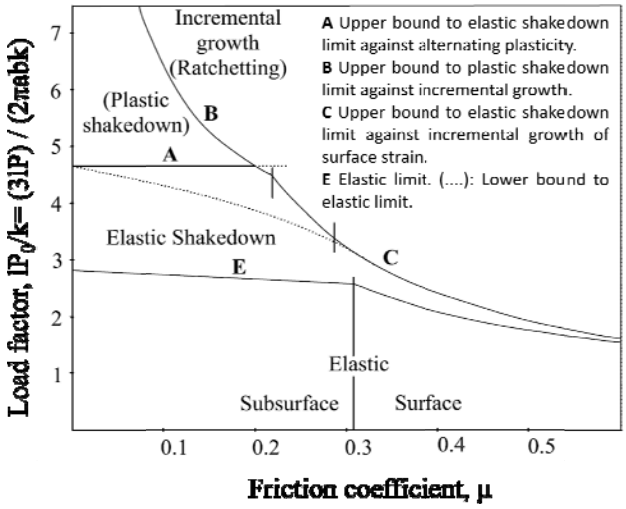

Fig. 7 A shakedown map for a general three-dimensional rolling-sliding contact

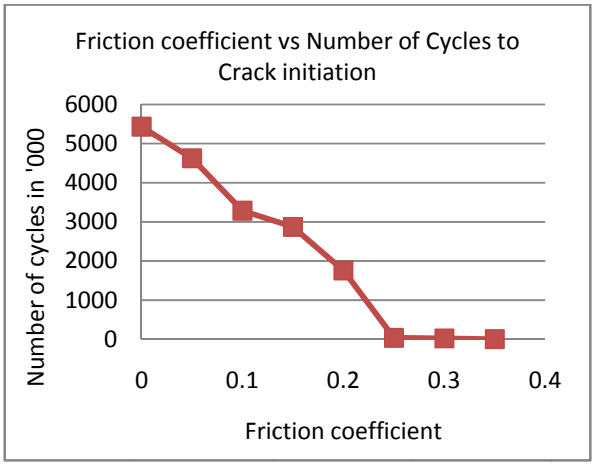

Fig. 8 A Graph of Friction coefficient vs. Number of cycles to Crack initiation

The subsurface damage due to low friction, as illustrated in Fig. 8, took a higher number of cycles to reach the defined damage criteria level in the critical element. Surface damage due to high friction took a small number of cycles to crack initiation.

VI. Conclusions

This paper presents a life prediction strategy for rolling contact fatigue crack initiation under ratchetting damage in rail contacts. It extends the critical crack plane concept [2] developed for rail/wheel contact by using multi cycle 3-D

elastic-plastic finite element analysis and significantly the critical element concept.

Therefore, the following conclusions can be made:

- Elastic-plastic FE analysis with critical element analysis is a valuable technique to predict fatigue life and crack initiation under ratchetting damage.
- The critical element concept provides a simple method to calculate the life-time to crack initiation compared to the previously developed criteria, such as critical plane concept.
- Recent tensile test data [25] and further cyclic loading testing means critical element concept can be applied to different materials in the future.
- Material models such as Jiang and Sehitoglu [26], [27] can be used with the new critical element concept to further define complex material behavior under cyclic loading.

Significantly, this work identified that at high friction forces, material failure is reached in a very short number of cycles, in the surface elements. This phenomenon is important to the rail industry in Australia as rail operators are increasing the high traction use of rail infrastructure.

VII. Acknowledgment

The authors are grateful to the Cooperative Research Centre for Rail Innovation (established and supported under the Australian Government's Cooperative Research Centres program) for the funding of this research: Project No. R3.110 Curve Lubrication.

References

[1] I. U. Wickramasinghe, D. Hargreaves, and D. D. Pellegrin, "The Suitability of Using Accumulated Plastic Strain to Assess the Damage at the Rail-Wheel Interfaces," in *J. Pombo, (Editor), "Proceedings of the First International Conference on Railway Technology: Research, Development and Maintenance"*, ed. Las Palmas de Gran Canaria, Spain: Civil-Comp Press, Stirlingshire, UK, Paper 95, 2012.

[2] J. W. Ringsberg, "Life prediction of rolling contact fatigue crack initiation," International Journal of Fatigue, vol. 23, pp. 575-586, 2001.

[3] J. W. Ringsberg, M. Loo-Morrey, B. L. Josefson, A. Kapoor, and J. H. Beynon, "Prediction of fatigue crack initiation for rolling contact fatigue," International Journal of Fatigue, vol. 22, pp. 205-215, 2000.

[4] J. Ringsberg, "Rolling contact fatigue of railway rails with emphasis on crack initiation," PhD Doctorate Thesis, Chalmers University of Technology, 2000.

[5] J. Ringsberg, H. Bjarnehed, A. Johansson, and B. Josefson, "Rolling contact fatigue of rails—finite element modelling of residual stresses, strains and crack initiation," Proceedings of the Institution of Mechanical Engineers, Part F: Journal of Rail and Rapid Transit, vol. 214, pp. 7-19, 2000.

[6] J. W. Ringsberg and B. L. Josefson, "Finite element analyses of rolling contact fatigue crack initiation in railheads," Proceedings of *the Institution of Mechanical Engineers, Part F: Journal of Rail and Rapid Transit,* vol. 215, pp. 243-259, July 1, 2001 2001.

[7] F. Franklin and A. Kapoor, "Modelling wear and crack initiation in rails," Proceedings of the Institution of Mechanical Engineers, Part F: Journal of Rail and Rapid Transit, vol. 221, pp. 23-33, 2007.

[8] A. Kapoor, F. J. Franklin, S. K. Wong, and M. Ishida, "Surface roughness and plastic flow in rail wheel contact," Wear, vol. 253, pp. 257-264, 2002.

[9] A. Kapoor, "Wear by plastic ratchetting," Wear, vol. 212, pp. 119-130, 1997.

[10] A. F. Bower and K. L. Johnson, "The influence of strain hardening on cumulative plastic deformation in rolling and sliding line contact," Journal of the Mechanics and Physics of Solids, vol. 37, pp. 471-493, 1989.

[11] A. F. Bower and K. L. Johnson, "Plastic flow and shakedown of the rail surface in repeated wheel-rail contact," Wear, vol. 144, pp. 1-18, 1991.

[12] Y. Jiang and H. Sehitoglu, "An analytical approach to elastic-plastic stress analysis of rolling contact," Journal of Tribology, vol. 116, p. 577, 1994.

[13] G. Schleinzer and F. D. Fischer, "Residual stress formation during the roller straightening of railway rails," International Journal of Mechanical Sciences, vol. 43, pp. 2281-2295, 2001.

[14] Y. Jiang, B. Xu, and H. Sehitoglu, "Three-Dimensional Elastic-Plastic Stress Analysis of Rolling Contact," *Journal of Tribology,* vol. 124, pp. 699-708, 2002.

[15] M. Ekh, A. Johansson, H. Thorberntsson, and B. L. Josefson, "Models for Cyclic Ratchetting Plasticity-Integration and Calibration," Journal of Engineering Materials and Technology, vol. 122, pp. 49-55, 2000.

[16] A. Johansson and H. Thorberntsson, "Elastoplastic material model with nonlinear kinematic hardening for rolling and sliding contact fatigue," Degree of Master of Science, Department of Solid Mechanics, Chalmers University of Technology, Gothenburg, Sweden, 1997.

[17] A. Bower, "Cyclic hardening properties of hard-drawn copper and rail steel," Journal of the Mechanics and Physics of Solids, vol. 37, pp. 455-470, 1989.

[18] Abaqus, Abaqus/CAE 6.9-1: © Dassault Systèmes, 2009.

[19] Y. Chen and J. Kuang, "Contact stress variations near the insulated rail joints," Proceedings of the Institution of Mechanical Engineers, Part F: Journal of Rail and Rapid Transit, vol. 216, p. 265, 2002.

[20] A. A. Shabana, K. E. Zaazaa, and H. Sugiyama, Railroad vehicle dynamics : a computational approach. Boca Raton: CRC Press, 2008.

[21] A. A. Shabana, K. E. Zaazaa, and H. Sugiyama, "Contact and Creep-Force Models," in Railroad Vehicle Dynamics, ed: CRC Press, 2007, pp. 127-159.

[22] J. L. Chaboche and J. Lemaitre, Mechanics of Solid Materials. Cambridge: Cambridge University Press, 1990.

[23] "Specification for railway rails," in BS 11:1985, ed, 1985.

[24] A. Kapoor, "A re evaluation of the life to rupture of ductile materials by cyclic plastic strain.," Fatigue & Fracture of Engineering Materials & Structures, vol. 17, pp. 201-219, 1994.

[25] T. Bandula-Heva and M. Dhanasekar, "Determination of stress-strain characteristics of railhead steel using image analysis," World Academy of Science, Engineering and Technology, vol. 60, pp. 1884-1888, 2011.

[26] Y. Jiang and H. Sehitoglu, "Modeling of Cyclic Ratchetting Plasticity, Part II: Comparison of Model Simulations With Experiments," Journal of Applied Mechanics, vol. 63, pp. 726-733, 1996.

[27] Y. Jiang and H. Sehitoglu, "Modeling of Cyclic Ratchetting Plasticity, Part I: Development of Constitutive Relations," Journal of Applied Mechanics, vol. 63, pp. 720-725, 1996.